

Optimality in kinetic proofreading and early T-cell recognition: revisiting the speed, energy, accuracy trade-off

Wenping Cui^{1,2} and Pankaj Mehta^{1,*}

¹*Department of Physics, Boston University, 590 Commonwealth Avenue, Boston, MA 02139*

²*Department of Physics, Boston College, 140 Commonwealth Ave, Chestnut Hill, MA 02467*

(Dated: September 20, 2022)

In the immune system, T cells can quickly discriminate between foreign and self ligands with high accuracy. There is significant evidence T-cells achieve this remarkable performance utilizing a network architecture based on kinetic proofreading (KPR). KPR-based mechanisms actively consume energy to increase the specificity beyond what is possible in equilibrium. An important theoretical question that arises is to understand the trade-offs and fundamental limits on accuracy, speed, and dissipation (energy consumption). Recent theoretical work suggests that it should always be possible to reduce the error of KPR-based mechanisms by waiting longer and/or consuming more energy. Surprisingly, we find that this is not the case and that there actually exists an optimal point in the speed-energy-accuracy plane for KPR and its generalizations. We give general arguments for why we expect this optimal to be a generic property of all KPR-based biochemical networks and discuss implications for our understanding of the T cell receptor circuit.

Keywords: Kinetic proofreading | immune decision | first-passage time | trade-off |

A central problem in immunology is the recognition of foreign ligands by the immune system. This process is carried out by specialized immune cells called T-cells which activate the immune response in the presence of foreign ligands. Foreign ligands are presented to T-cells by specialized Antigen Presenting Cells (APCs) that bind a repertoire of self and foreign peptides. T-cells activation occurs when specialized receptors on the surface of T-cells, called T-cell receptors (TCRs), bind APCs, and activate downstream the TCR signaling network, leading to an immune response.

It has been shown that T-cells have a high sensitivity to foreign ligands. A few foreign ligands (less than 10) appearing on the membrane of a T-cell are able to trigger the immune response[1, 2]. Moreover, this decision is made extremely quickly: it only takes 1-5 mins to make the decision to activate or not [3]. Despite the speed with which the response is mounted, T-cells can accurately sense the existence of foreign ligands with an error rates as small as $10^{-4} - 10^{-6}$ [4, 5]. This raises natural questions about how the T-cell signaling network can operate with such high speed, sensitivity, and accuracy.

Experimental evidence suggests that T-cell activation is set by the binding time of the antigen-receptor complex [6, 7]. If the binding time of the ligand to the receptor is below a sharp threshold (3-5 sec), T-cells do not activate. However if the binding time is above this threshold, T-cells activate with extreme sensitivity. This so called ‘life-time’ dogma places stringent conditions on the machinery of the immune response[6]. A lot is known about the biochemical networks that implement this thresholding procedure. The receptor-ligand complexes go through multiple rounds of phosphorylation (throughout we denote the number of phosphorylations by n). Within the life-time dogma, an immune response is triggered if the concentration of the ligand-receptor complex that has been phosphorylated n times exceeds a threshold con-

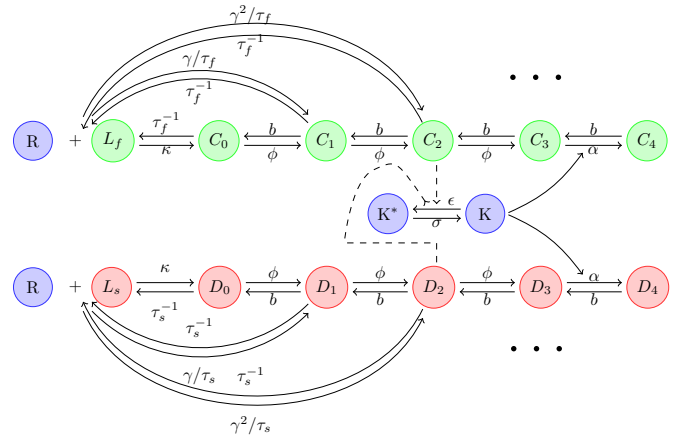


FIG. 1. Schematic overview of a kinetic proofreading network. Products from foreign ligands C and self ligands D decay to free R and free L_i with a different rate τ_f^{-1} and τ_s^{-1} respectively. A reversible processes are considered with a reversible decay rate γ^n/τ_i ($i = s, f$). The definition of symbols can be found at Table. I.

centration.

The ability of T-cells to discriminate between foreign and self ligands arises from the difference in the binding times of foreign (τ_f) and self (τ_s) ligands[8]. Typically, in the immune system, $\tau_s \sim 1s$ and $\tau_f \sim 10s$. In equilibrium, this binding time difference cannot account for the incredible accuracy of the T-cell immune response. Detailed balance places constraints on the chemical reaction rates and the reliability of the discrimination process is ultimately limited by equilibrium thermodynamics[9]. This binding time difference can be directly translated into a difference in binding free energies of foreign and self ligands [10, 11]. Thus, a biochemical network that works at equilibrium can achieve a minimum error rate

of $\tau_s/\tau_f \sim 0.1$, nearly three orders of magnitude smaller than that seen in experiments.

It is known the immune system can beat this bound by working out-of-equilibrium and consuming energy[4]. It is now thought that the T-cell employs a form of kinetic proofreading(KPR), first proposed by Hopfield[10] and Ninio[11]. But current understanding of KPR and its implications for immune response have several weaknesses: firstly, most theoretical treatments of KPR involve approximating certain reactions as irreversible making it difficult to consistently calculate energy consumption; second, it is extremely hard for KPR-based schemes to simultaneously distinguish ligands with similar binding times and operate over a large dynamic range of ligand concentrations. The later shortcoming has been addressed by a generalization of KPR called ‘‘adaptive sorting’’. In adaptive sorting, an additional feedback couples the KPR cascades in the T-cell through a common kinase that regulates all the phosphorylation of all T-cell receptors [7, 12–15].

A fundamental issue in the study of T-cell activation is to understand the trade-off between different functionalities – accuracy, speed and dissipation – in the immune discrimination process. Many works have studied the relation between accuracy and dissipation or accuracy and speed for some KPR-based biochemical network[16–22]. Some others have discussed general error rate bounds under power constraints in the context of thermodynamics or information theory[23–28]. Few works[29, 30] consider the trade-off between these three quantities simultaneously. These theoretical work suggests that it is always possible to reduce the error of KPR-based mechanisms by waiting longer and/or consuming more energy [16, 20].

In this paper, we calculate the speed, power dissipation, error rate and output signal (the combined concentration of D_N and C_N) explicitly for a KPR-based biochemical network, with and without a feedback that implements adaptive sorting (shown in Fig. 1). We ask if there is an optimal operating point for T-cell activation networks where T cells can make fast and accurate decisions while utilizing energy efficiently. Surprisingly, we find that such an optimal point exists for KPR and its generalizations. Near the optimal point, the response time and power dissipation are consistent with those observed in experiments, implying that many mechanisms of early T-cell recognition are well described by KPR-based models.

I. MODEL

We start from the adaptive sorting model shown in Fig. 1 [7, 13–15]. The receptor, R , can bind a foreign or self ligand, to form a complex C_0 and D_0 respectively. This complex can be phosphorylated a maximum of N times. We denote a receptor-ligand complex that has been phosphorylated n times by X_n with $X = C$ for foreign ligands and $X = D$ for self ligands. The dynamics of the bio-

chemical network can be written as:

$$\begin{aligned}\dot{X}_0 &= \kappa R L_i - (\tau_i^{-1} + \phi) X_0 + b X_1 \\ \dot{X}_n &= \gamma^n R L_i / \tau_i + \phi X_{n-1} - (\phi + \tau_i^{-1} + b) X_n + b X_{n+1} \\ \dot{X}_N &= \gamma^N R L_i / \tau_i + \alpha K X_{N-1} - (b + \tau_i^{-1}) X_N \\ \dot{K} &= -\epsilon K (C_m + D_m) + \sigma (K_T - K)\end{aligned}\quad (1)$$

where $N > n > 0$, $X \in \{C, D\}$, and $i \in \{f, s\}$. $R = R_T - \sum_{j=0}^N (C_j + D_j)$ and $L_i = L_i^T - \sum_{j=0}^N X_j$ are the free concentration of receptors and ligands, with R_T , L_T and K_T the total number of receptors, ligands and kinase respectively. For notational simplicity, throughout the manuscript we assume that cell volume is fixed and hence do not distinguish between species number and concentration. In Fig. 1, we set $N = 4$ and $m = 2$. More information about molecular species and notation can be found in Table. I.

In the adaptive sorting network, both foreign and self ligands can bind a receptor and form the receptor-ligand complex, X_0 , which can undergo multiple rounds of phosphorylation (X_n goes to X_{n+1}) and dephosphorylation (X_n goes to X_{n-1}). The receptor-ligand complexes can disassociate (at a rate τ_s^{-1} for self ligands and τ_f^{-1} for foreign ligands). During this process, the phosphate groups are lost and the whole process reinitiates. Importantly, once a ligand is bound to a receptor, it is impossible for the biochemical machinery to distinguish between foreign and self ligands. The binding rate κ , the phosphorylation rate, ϕ , and the dephosphorylation rate, b , inside the cell are the same for the foreign and self ligands and the only difference between foreign and self ligands are the lifetimes of their corresponding receptor-ligand complexes. For this reason, the decision to activate is based on the concentration of the total final products $C_N + D_N$ from both the foreign ligand (C_N) or self ligand (D_N).

In the adaptive sorting network, in addition to the phosphorylation cascade, a negative feedback is used to modulate the phosphorylation and/or dephosphorylation rates [7, 13]. For example, in Fig. 1 the last phosphorylation step, from X_{N-1} to X_N , is modulated by the level of active kinase K , which itself is dependent on the concentration of the m -th intermediate concentration X_m through phosphorylation. With this feedback, the output signal is independent of the ligand concentration and only replies on the value of τ . This model reduces to a KPR cascade when the feedback is absent, *i.e.* $\epsilon = 0$ and $\alpha = \phi/K_T$.

In most treatments of KPR, the disassociation of the receptor-ligand is often treated as an irreversible process ($\gamma = 0$). Often, this is a good approximation since phosphatases can easily bind free receptors and quickly remove phosphate groups from the receptors [4]. However, in any thermodynamically consistent model, all reactions are reversible and it is important to consistently treat both the forward rate and backward rate for the formation and disassociation of a complex. For this reason, we introduce a small rate, $\gamma_{n,i} = \gamma^n / \tau_i$ ($i = s, f$), for directly

TABLE I. Definition of symbols shown in Fig. 1

Symbol	Definition
C_n	Agonist complex phosphorylated n times
D_n	Non-agonist complex phosphorylated n times
R	Receptor
K	Active kinase
K^*	Inactive kinase
K_T	Kinase
ϕ	Complex phosphorylation rate
αK	Complex phosphorylation rate at the final step
b	Complex dephosphorylation rate
σ	Kinase phosphorylation rate
ϵ	Kinase dephosphorylation rate

forming a complex C_n and D_n (see Supporting Information). This functional form is a direct consequence of assuming that there is a constant free energy difference $k_B T \log \phi / \gamma b$ per phosphorylation. Furthermore, we assume this rate is small ($\gamma \ll 1$). Below, we show that taking $\gamma \neq 0$ is essential to obtain the optimal point in the speed-energy-accuracy plane.

II. DEFINING ACCURACY, SPEED, AND DISSIPATION

Before analyzing the biochemical network outlined above, it is necessary to define accuracy, energy consumption, and speed for T-cell recognition in greater detail.

A. Accuracy

Recall, that a T-cell makes the decision to activate based on the total concentration of the full phosphorylated complexes $C_N + D_N$ from both the foreign ligand (C_N) and self ligand (D_N). Ideally, T-cells are activated only in response to foreign ligands. Thus, following Hopfield [10] we can define the error rate η as the ratio of C_N and D_N :

$$\eta = \frac{D_N}{C_N}. \quad (2)$$

The concentrations of different components can be calculated by solving the deterministic equations (1) at steady state. In the immune recognition by T cells, it is important to achieve a small error rate $\sim 10^{-4} - 10^{-6}$. For an irreversible N -step KPR process (i.e. $\gamma = 0$), η can reach a minimum value we dub the ‘‘Hopfield limit’’

$$\eta_{min} = \tau_s^N / \tau_f^N. \quad (3)$$

We define the accuracy as one minus the error rate, $1 - \eta$.

B. Energy Consumption

In any non-equilibrium steady state, detailed balance is broken and leading to the existence of net currents in

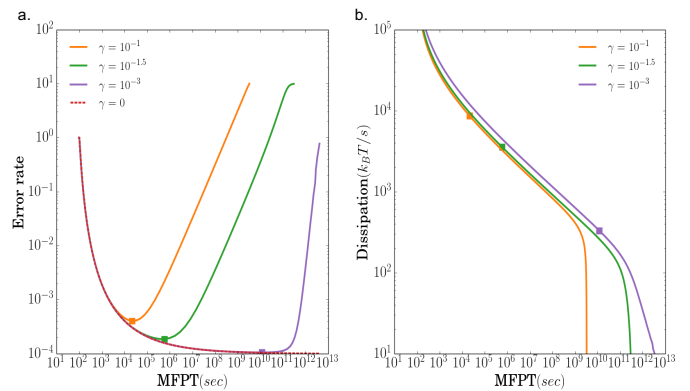


FIG. 2. Effects of γ in KPR: $\tau_s = 1s$, $\tau_f = 10s$, we change ϕ but keep $b/\phi = 0.01$ fixed. The solid lines are for $\gamma = 0.1, 10^{-1.5}, 10^{-3}$ and 0. (a): relation between accuracy and mean first-passage time (1/speed); (b): relation between dissipation (power consumption) and mean first-passage time (1/speed). The squares indicate locations of the correspond minimal error rate.

the network[23, 31]. The chemical potential difference between the reactants and products can be written as

$$\Delta\mu = k_B T \ln \frac{J_+}{J_-} \quad (4)$$

where J_+, J_- are forward- and backward-reaction fluxes. The net current is $J = J_+ - J_-$. The power dissipation is defined as [31, 32]

$$W = k_B T J \ln \frac{J_+}{J_-} \quad (5)$$

For example, the power dissipation of the first-step phosphorylation process: $C_0 \xrightarrow[b]{\phi} C_1$ can be calculated as:

$$W = k_B T (\phi C_0 - b C_1) \ln \frac{\phi C_0}{b C_1} \quad (6)$$

This can be generalized to the full KPR cascade and adaptive network (see Supporting Information). Finally, we adapt the convention of nonequilibrium thermodynamics and use the phrases ‘‘energy consumption’’ and ‘‘power dissipation’’ interchangeably.

C. Speed

The speed of decision-making process is related to the mean first passage time(MFPT) of a stochastic process[33]. The MFPT is defined as average the time taken to produce one molecule of the final product C_N from the foreign ligand L_f . For example, at each time step, one molecule of the complex C_3 can be phosphorylated at a rate ϕ to yield C_4 , or can be dephosphorylated at a rate b to get a molecule to C_2 , or alternatively decay rate τ_f^{-1} to yield a free receptor R . Microscopically, this

can be viewed a stochastic process – similar to a random walk– and different realization of this process will take different amounts of time. The MFPT is taken as the average time it takes to complete to get from the starting point to the target. We use the mean MFPT to define the inverse of the decision speed. Detailed calculation procedures can be found in Supporting Information and [34].

Calculating speed in the adaptive sorting network is technically much more challenging than in KPR due to the non-linearity introduced by the additional feedback loop. To overcome this difficulty, we employ a linear-response approximation around the steady-state operating point when calculating the speed. Such linear-response approximations are commonly employed in engineering (e.g. gain, bandwidth) and have been adapted with great success to analyze biochemical circuits [35]. In the linear-response regime of adaptive sorting, the MFPT can be calculated using methods analogous to KPR (see Supporting Information and [36, 37]).

Finally, we note that in a related work, the speed is associated with the inverse of the smallest eigenvalue of the master equation describing the biochemical circuit[30]. However, it has been shown that this definition is not a good measure of speed unless one considers long Markov chains (i.e. $N \rightarrow \infty$) dominated by nearest-neighbor transitions [38]. The circuits considered here operate very far from these regimes.

III. RESULTS

We now analyze the speed-energy-accuracy tradeoff in KPR and adaptive-sorting circuits. One difficulty involved in identifying general principles are the large number of parameters whose choice can dramatically change the properties of the underlying circuit (see Table. I). For this reason, we will take a strategy based on randomly sampling these parameters in numerical simulations and looking for accessible regions in the energy-speed-accuracy plane. This spirit is similar to the one used to identify robustness in the adaptation circuit of bacterial chemotaxis [39, 40]. We begin by analyzing a KPR cascade where the feedback loop from the kinase K in Fig. 1 is turned off and then subsequently extend our analysis to the full adaptive sorting network.

A. Kinetic proofreading

Recent theoretical work suggests that it is always possible to reduce the error of KPR-based mechanisms by waiting longer and/or consuming more energy[20]. Surprisingly, we find that this is not the case. Our results show the error rate increases dramatically at extremely slow speeds/low dissipation when γ (the rate to directly form a complex) has a nonzero value.

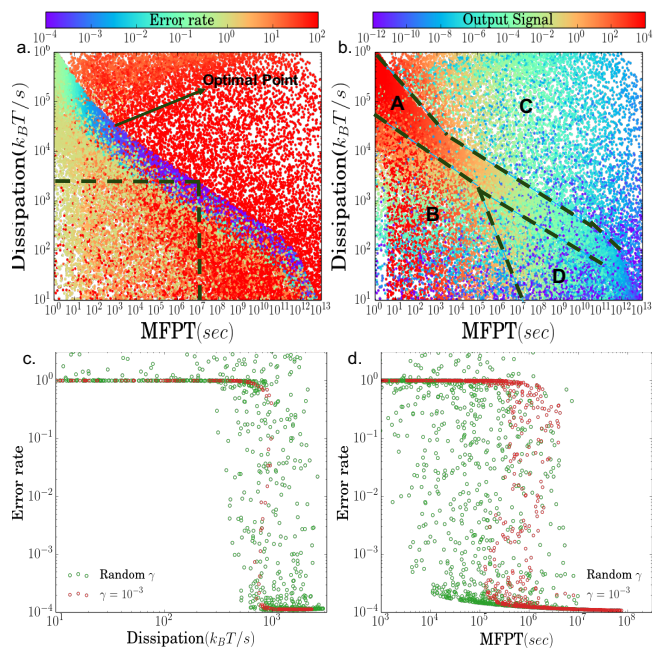


FIG. 3. Plots of the error rate and the magnitude of the output signal as a function of the mean first-passage time (1/speed) and dissipation (power consumption) for randomly sampled parameters (a) Error rate; (b) Output signal: $C_4 + D_4$; (c) Error rate versus dissipation for a fixed time = 10^7 s corresponding to the vertical dashed line in (a); (d) Error rate versus mean first passage time (inverse speed) at fixed dissipation rate = $10^{3.2} k_B T$ corresponding to the horizontal dashed line in (a). The optimal point with high accuracy, high speed, low-dissipation, and a large output signal is labeled in (a). The behavior of circuit can be classified into four distinct regions labeled in A-D (see main text for more details).

We studied the effects of varying γ with numerical simulations shown in Fig. 2. When $\gamma = 0$, waiting longer always decreases the error rate. As shown in Fig. 2(a), the error rate η monotonically decreases with the MFPT (1/speed) and asymptotically reaches the Hopfield limit for an infinitely slow circuit: $\tau_s^N / \tau_f^N = 10^{-4}$ for a circuit with $N = 4$ phosphorylations. In this high accuracy regime, a ligand must bind the receptor multiple times and transverse all N steps of the phosphorylation cascade before reaching the final products X_N . However, when $\gamma \neq 0$, for sufficiently long times, the probability to directly form a phosphorylated complex and bypass the initial kinetic proofreading steps becomes non-negligible. This leads to an increase in the error rate [10, 20]. Thus, increasing γ drives a cross-over in the dynamic behavior of the biochemical circuit from a regime where waiting longer increases the accuracy to one where waiting longer decreases the accuracy. We also investigated the relationship between the speed of the circuit and power consumptions. Fig. 2(b) shows that over large parameter regime, the energy consumption and MFPT (1/speed) exhibit an approximate power law (linear relationship on a log-log plot). This indicates that making a decision quickly al-

ways requires a large amount of energy consumption. This approximate power-law relationship breaks down for extremely slow circuits.

In order to better understand the relationship between speed, accuracy, and energy consumption, we randomly sampled different combinations of the three parameters: ϕ , b , γ and calculated all three quantities (see Supporting Information for details). The results are shown in the Fig. 3(a). We also calculated the total output signal (the concentration of $C_N + D_N$) for each parameter set Fig. 3(b). In both plots, each point corresponds to a different choice of the parameters.

To better understand these plots, it is helpful to separate the parameters into four qualitatively distinct operating regimes (see Fig. 3): (A) a high-accuracy regime, (B) a high-speed, low-dissipation, low-accuracy regime, (C) a high-dissipation, low-accuracy regime, and (D) a low-dissipation, low-speed, low-accuracy regime.

One of the most dramatic features in Fig. 3(a) is the blue, high-accuracy region A. In Region A, the error rate of the KPR cascade approaches its theoretically minimum possible value (i.e. the ‘‘Hopfield Limit’’) $\eta_{min} = \tau_s^N / \tau_f^N \approx 10^{-4}$. This high accuracy region is realized when $\gamma \ll 1$, $b/\phi \ll 1$ and $\phi \ll \tau_s^{-1}$. These parameter regimes corresponds to the assumptions outlined by Hopfield as being necessary for achieving high-accuracy proofreading [10]. Many choices of parameters in Region A achieve this high accuracy. However, as shown Fig. 3(b) for many of these choices of parameters the magnitude of the output signal is quite small. This motivates defining an optimal operating point of the KPR regime as the choice of parameters with highest accuracy and a high output signal. This point is marked as the optimal point in Fig. 3(a). We discuss this optimal point extensively below.

In Region B, one can make a fast decision speed with minimal energy consumption, but the error rate is well above the Hopfield limit. Here, $b/\phi \ll 1$ and $\phi \gtrsim \tau_s$. In this parameter regime, there is a steady- flux of empty receptors that are converted to the fully phosphorylated output complex. The MFPT is reduced but the system becomes insensitive to the difference between foreign and self-ligand binding times: the forward rate is so large that there is no time for the intermediate complexes to decay making it impossible to distinguish τ_s^{-1} and τ_f^{-1} . Region C has the highest error rate. Here, $\gamma \gtrsim 1$, $b/\phi \gg 1$ and $\phi \gtrsim \tau_s$. For such large values of γ , there is a continuous flux from free receptor directly to the fully-phosphorylated complex $C_N(D_N)$, with most output molecules bypassing the proofreading steps. In this region, $\gamma \geq \tau_f^{-1}, \tau_s^{-1}$ is much bigger than the binding times of ligands resulting in error rates that can be as large as $\eta = \tau_f^2 / \tau_s^2 = 100$ (see Supporting Information). In practice, for reasonable values of γ (e.g. $\gamma \ll 1$), no biochemical networks operate in region C. Finally, in region D, speed decreases dramatically because of $\gamma \ll 1$, $b/\phi \gg 1$.

Figure 3c and d show cross-sections of the error rate

for a fixed speed and fixed dissipation rate respectively. These graphs were generated by selecting all parameters that lie along the vertical and horizontal dashed lines in Fig. 3a. One of the most striking aspects of these plots is how dramatically the error rate decreases from the ‘‘equilibrium value’’ of $\tau_s / \tau_f = 0.1$ to the theoretical maximum ‘‘Hopfield limit’’ $\left(\frac{\tau_s}{\tau_f}\right)^4 = 10^{-4}$ as a function of the dissipation rate and mean first-passage time. Furthermore, the transition between these values become steeper and narrower as γ is reduced. These plots suggest that for slow speeds (above $\sim 10^{-7} s^{-1}$) and low dissipation rates (below $\sim 10^3 k_B T/s$) there is likely a dynamic phase transition in the KPR circuit when either the dissipation rate or speed is held fixed and other parameters are varied.

Murugan and collaborators have argued that KPR has a natural mapping to microtubule growth, a system with a known dynamical phase transition between growth and shrinkage, and it has been argued that such a transition is also likely to be a generic feature of KPR [20]. However, unlike the systems analyzed by [20], we consider a non-zero transition rate, γ , which leads to qualitatively different results. In particular, when the mean first-passage time become comparable to the typical time it takes to ‘‘bypass’’ the KPR steps and directly form the complex C_2 , set by τ_f / γ^2 (see Fig. 1). This leads to the low-fidelity region C in Fig. 3 and accounts for the existence of the optimal point in the speed-accuracy-dissipation plane.

B. Extending our results to adaptive sorting

In the preceding section, we have focused on the speed, accuracy, and dissipation trade-offs in a simple KPR cascade. Adaptive sorting is a very promising extension of KPR relevant for understanding T-cell activation in immune recognition [7, 13–15]. Adaptive sorting employs an additional negative feedback loop in the last step of the KPR cascade that ensures the output signal is independent of the number of ligands in the environment. This ability to perform ‘‘absolute ligand discrimination’’ is a key feature of adaptive sorting. It accounts for how a T-cell can achieve high accuracy in natural environmental conditions where the concentration of self-ligands is large and dwarfs the concentration of foreign ligands ($C_m \gg D_m$ and $C_m \gg 1$). A natural question is to ask if there is any tradeoffs involved needed to achieve absolute ligand discrimination. One such tradeoff is antagonism, where increasing the concentration of foreign ligands actually degrades the response of the adaptive sorting circuit [41]. We show here that there is another tradeoff between absolute ligand discrimination and the speed at which the T-cell receptor circuit can operate.

Figure 4 shows error rate, mean first-passage time, and dissipation rate of the adaptive sorting and the KPR cascade analyzed above with regards to the tradeoffs between speed-accuracy and dissipations. The dissipation

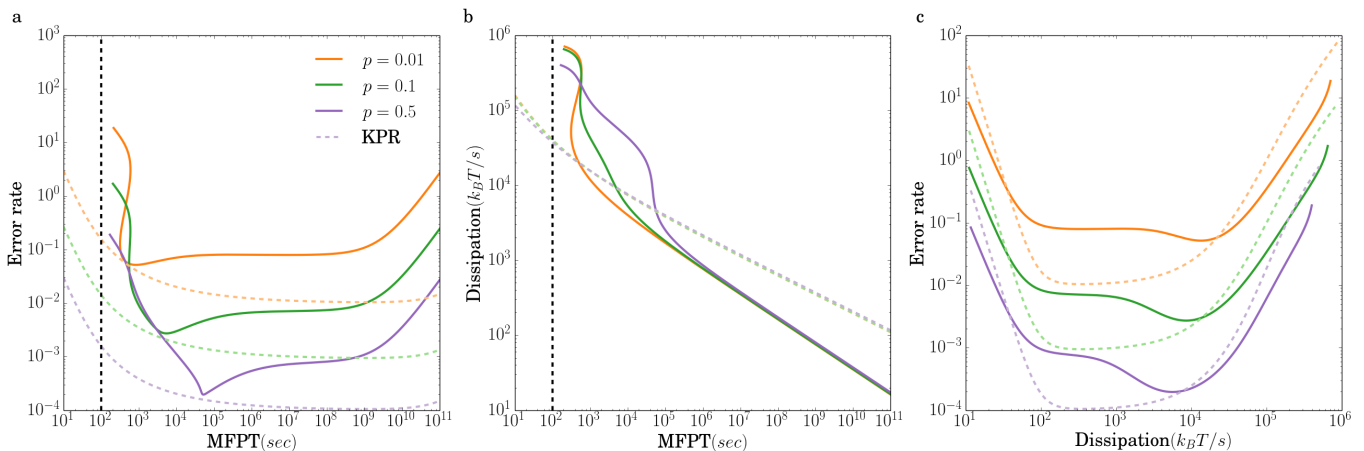


FIG. 4. Effects of changing proportions of foreign ligand p on the relations between Time, Dissipation and Error rate for adaptive sorting process. $L_T = 2.0 \times 10^4$, $L_f = pL_T$, $L_s = L - L_f$. $K_T = 10^3$, $\gamma = 10^{-3}$, $\sigma = 2s^{-1}$, $\epsilon = 1s^{-1}$, $\alpha K_T = 3 \times 10^{-1} s^{-1}$. The dashed lines are KPR results corresponding to different p . The black, vertical dashed line marks indicates the experimentally-measured time it takes T-cells to make decisions.

and error rate of the adaptive sorting model is comparable to a KPR cascade. However, from Fig. 4(a,b), it takes the adaptive sorting circuit much longer to achieve a similar error rate as a KPR. For a very large input signal, the phosphorylation rate of the last step in the cascade is dramatically decreased, leading to dramatic decrease in speed because most complexes fall apart before reaching the final step of the cascade. Furthermore, notice that unlike KPR, the adaptive sorting circuit is unable to achieve even modest error rates for mean first passage times of 100s (vertical dashed lines in Fig. 4), corresponding to the experimentally observed time it takes T-cells to make the activation decision.

IV. DISCUSSION

The immune system must quickly and accurately recognize foreign ligands. To carry out this task, the T-cells work out of equilibrium by actively consuming energy. This raises natural questions about the relationship between speed, accuracy, and energy consumption in two classes of biochemical networks that have been used to model immune recognition: a KPR-based network and a generalization of KPR, adaptive sorting. Importantly, unlike previous work, we made no approximation about the underlying parameter space and this allowed us to identify an optimal operating point in the speed-energy-accuracy plane. We also found that the behavior of these networks exhibit four different regimes, which surprisingly included a fast, high-accuracy regime at intermediate energy consumption.

Our results stand in contrast with recent theoretical work suggesting that it may always be possible to achieve a better accuracy by waiting longer or consuming more energy. The underlying reason for this is that unlike these previous works we allow for a tiny (but) non-zero rate for

bypassing the proofreading steps. This non-zero rate is necessary in any thermodynamically consistent model. While the parameter has no effect at short times, for very long times the error increases because the probability of bypassing the proofreading steps becomes significant. The generality of this argument suggests that our conclusions should also hold for other, more complicated biochemical networks.

It has been argued that a KPR-based T-cell activation is likely to fail when the concentration of external ligands becomes large and one must instead consider an adaptive sorting based circuit [7, 13–15]. Unlike a simple KPR cascade, the adaptive sorting network can distinguish between foreign and self even for large ligand concentration, a property dubbed “absolute ligand discrimination”. We have found that absolute ligand discrimination comes at a large cost in speed compared to a simple KPR-based circuit.

We can compare our results for speed accuracy, and energy consumption to experiments. T-cells spend 1-5 mins to make the decision to activate [6]. A rough estimation of the error rate from experiment suggests cells can achieve error rates in the range $10^{-4} - 10^{-6}$ or smaller, with the exact number depending on properties of ligands [4, 5]. The energy expended by a T-cell to make the activation decision is hard to measure directly. However, estimates of the power consumption from glucose consumption suggest a typical cells uses about 10^9 ATP/s [42, 43]. These numbers set strict experimentally-derived bounds for our model.

For a circuit with $N = 4$ phosphorylations, the minimum error rate achieved by both KPR and adaptive sorting is 10^{-4} , on par with the experimental error rates. As shown in Fig. 4, the KPR cascade can achieve close to this optical accuracy in the experimentally observed decision time of 100s. The power consumption of the circuit is $W \sim 1000$ ATP/s (where we have used the standard

conversion $1\text{ATP} = 14 - 15k_B T$ [44]), just one-one thousandth of the total energy budget of the cell. Moreover as shown in Fig. S12 (see Supporting Information), increasing the number of steps in the phosphorylation cascade N can significantly increase the accuracy of a KPR cascade with only modest decreases in the speed and the magnitude of the output signal. An adaptive sorting circuit can also reach the optimal error rate of 10^{-4} using approximately the same energy budget as a simple KPR cascade. However, the absolute ligand discrimination of adaptive sorting comes at a steep price in terms of speed. For the biologically realistic 100s window for making immune recognition, the KPR cascade achieves a respectable error rate between 10^{-3} and 10^{-4} whereas the adaptive sorting circuit is essentially non-functional.

More generally, the trade-off between speed, accuracy, and power consumption in realistic biochemical networks is still poorly understood. Our results based on a simple model of immune decisions show that thermodynamics places strict constraints on these non-equilibrium processes. Energy consumption is required to maintain these non-equilibrium processes. With extremely low energy consumption or slow speed, the decision signal will be ruined by thermal fluctuations. However, when operating in regimes with extremely large energy consumption or speed, subtle effects can suddenly transition circuits so that decisions are dominated by rare events that destroy accuracy. This suggests that great care is needed in both

modeling and/or engineering KPR-based decision making circuits.

One of the most striking aspects of our simulations are the sudden transitions in accuracy as a function of the dissipation rate (at fixed speed) or speed (at fixed dissipation). These transitions seem to be indicative of an out-of-equilibrium dynamic phase transition. In the future, it will be interesting to further investigate this transition and see if it is possible to adopt analytic methods and fluctuation-type theorems to better understand its origins. Our work also suggests that it is extremely difficult for adaptive sorting networks to simultaneously perform absolute ligand discrimination and operate quickly. An important area of future work is to better understand if this trade-off is fundamental or can be bypassed with more clever network architectures. Finally, it will be interesting to explore general networks and develop analytic techniques to further our understanding of optimal operating points with regards to speed, accuracy, and power consumption.

ACKNOWLEDGMENTS

This work was supported by NIH NIGMS MIRA grant number 1R35GM119461 and Simons grant in the Mathematical Modeling of Living Systems to PM.

Appendix A: Definition of Model and parameter choices

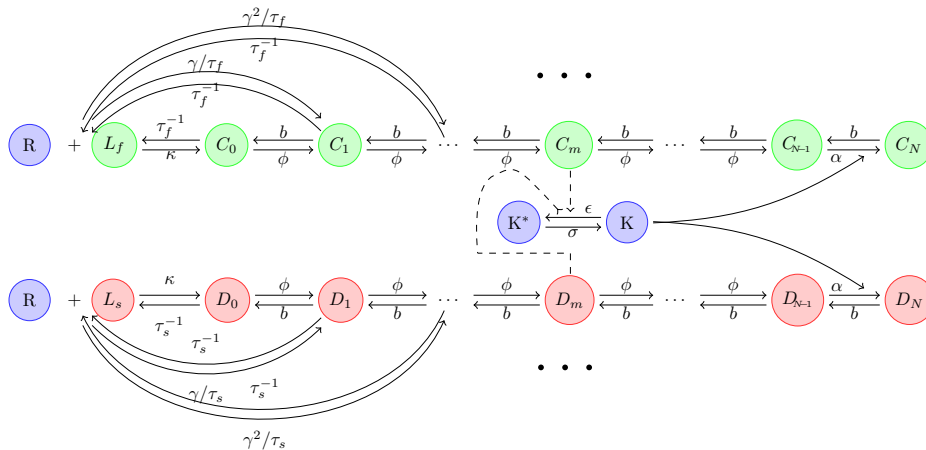


FIG. 5. Schematic overview of a general kinetic proofreading network.

A schematic of the model we are considering is shown in Fig. 5. As described in the main text, we denote a receptor-ligand complex that has been phosphorylated n times by X_n with $X = C$ for foreign ligands and $X = D$ for self ligands. Furthermore, we denote the maximum number of phosphorylations as N . With this notation, using the

law of mass action, we have

$$\begin{aligned}
\dot{C}_0 &= \kappa RL_f - \left(\tau_f^{-1} + \phi\right) C_0 + bC_1 \\
\dot{C}_n &= \gamma^n RL_f / \tau_f + \phi C_{n-1} - (\phi + \tau_f^{-1} + b) C_n + bC_{n+1} \\
\dot{C}_N &= \gamma^N RL_f / \tau_f + \alpha K C_{N-1} - (b + \tau_f^{-1}) C_N \\
\dot{K} &= -\epsilon K (C_m + D_m) + \sigma (K_T - K) \\
\dot{D}_0 &= \kappa RL_i - \left(\tau_s^{-1} + \phi\right) D_0 + bD_1 \\
\dot{D}_n &= \gamma^n RL_i / \tau_s + \phi D_{n-1} - (\phi + \tau_s^{-1} + b) D_n + bD_{n+1} \\
\dot{D}_N &= \gamma^N RL_s / \tau_s + \alpha K D_{N-1} - (b + \tau_s^{-1}) D_N
\end{aligned} \tag{A1}$$

where $N > n > 0$, $R = R_T - \sum_{j=0}^N (C_j + D_j) \sim R_T$, $L_s = L_s^T - \sum_{j=0}^N D_j$ and $L_f = L_f^T - \sum_{j=0}^N C_j$. Typically, we set: $R_T = 10^4$, $L_f^T = L_s^T = 10^4$, $\kappa = 300s^{-1}$, $\sigma = 1s^{-1}$, $\epsilon = 2s^{-1}$, $K_T = 10^4$, $\alpha = 3 \times 10^{-4}$, $\gamma = 10^{-3}$, $\tau_s = 1s$ and $\tau_f = 10s$. Any deviations from this choice of parameter is explicitly noted.

1. Accuracy

At steady state, the error rate can be written as

$$\eta = \frac{D_N}{C_N} \tag{A2}$$

In the presence of the kinase feedback $K = \frac{\sigma K_T}{\sigma + \epsilon(C_2 + D_2)}$, the set of eqs. (A1) are no longer linear and but the steady-state solution can still be found easily using an iterative method.

2. Energy Consumption

The power dissipation is calculated based on the net flux and the chemical potential difference[31, 32]. We define the net flux $J_{\alpha,n}$, $i \in [s, f]$ at $X_n \rightleftharpoons X_{n+1}$ in the main pathway.

$$J_{i,n} = \begin{cases} \phi X_n - bX_{n+1}, & \text{for } 0 \leq n < N - 1 \\ \alpha K X_{N-1} - bX_N, & \text{for } n = N \end{cases}$$

Considering the flux conservation, the power dissipation P_i can be written as

$$\begin{aligned}
P_i &= k_B T J_{i,0} \ln \frac{\kappa RL_i^{free}}{\tau_i^{-1} X_0} + k_B T \sum_{n=0}^{N-2} J_{i,n} \ln \frac{\phi X_i}{b X_{i+1}} + k_B T J_{i,N-1} \ln \frac{\alpha K X_{N-1}}{b X_N} \\
&+ k_B T \sum_{n=0}^{N-2} (J_{i,n} - J_{i,n+1}) \ln \frac{X_{n+1}}{\gamma^{n+1} RL_i^{free}} + k_B T J_{i,N-1} \ln \frac{X_N}{\gamma^N RL_i^{free}} \\
&= k_B J_{i,0} \ln \frac{\kappa}{\tau_i^{-1}} + k_B T \sum_{n=0}^{N-2} J_{i,n} \ln \frac{\phi}{b \gamma} + k_B T J_{i,N-1} \ln \frac{\alpha K}{b \gamma}
\end{aligned}$$

The total power dissipation is from the contribution of both foreign and self ligands: $P = P_s + P_f$.

3. Role of γ

In KPR, the reversible decay rate is ignored as it has extremely small value. However, from thermodynamics and calculation for energy consumption, we have to include it into our model. One choice of the reversible decay rate is γ^n / τ_i . There are two reasons for this form: 1. the production rate from ligands and receptors to X_{n+1} should be smaller than the one to X_n as one more phosphorylation step is involved; 2. it is also natural to assume the energy consumption is the same for each phosphorylation step.

The free energy difference between n th and $n+1$ th phosphorylation round can be calculated as:

$$\begin{aligned}\Delta G_n &= k_B T \log \left[\frac{\kappa}{\tau_i^{-1}} \frac{\phi^{n+1}}{b^{n+1}} \frac{\tau_i^{-1}}{\gamma^{n+1}/\tau_i} \right] - k_B T \log \left[\frac{\kappa}{\tau_i^{-1}} \frac{\phi^n}{b^n} \frac{\tau_i^{-1}}{\gamma^n/\tau_i} \right] \\ &= k_B T \log \frac{\phi}{\gamma b}\end{aligned}\quad (\text{A3})$$

4. Speed

The speed is defined by the mean first passage time(MFPT) for the foreign ligand. Here we mainly follow the procedures in Ref. [34]. The concentration vector is defined as $\mathbf{c} = [L_f, C_0, C_1, \dots, C_N, p_f]$. An final 'dark' state is added because the response is only activated at the end and it can be treated as absorbing markov chain. Added this absorb state, it becomes an irreversible process, which is impossible to calculate the energy consumption. The transfer probability from C_N to the 'dark' state is W (irreversible). We set $W = 100s^{-1}$, a large value, which means the final step has little effect on MFPT. Without loss of generality, we begin with $N = 4$ and $m = 2$, which can be generalized other cases easily. The master equations *i.e.* eqs. (A1) can be rewritten as $\dot{\mathbf{c}} = \mathbf{A}\mathbf{c}$ and

$$\mathbf{A} = \begin{bmatrix} -\kappa R - \sum_{j=1}^4 \gamma^j / \tau_f & \frac{1}{\tau_f} & \frac{1}{\tau_f} & \frac{1}{\tau_f} & \frac{1}{\tau_f} & \frac{1}{\tau_f} & 0 \\ \kappa R & -\frac{1}{\tau_f} - \phi & \frac{1}{b} & 0 & 0 & 0 & 0 \\ \gamma / \tau_f & \phi & -\phi - \frac{1}{\tau_f} - b & b & 0 & 0 & 0 \\ \gamma^2 / \tau_f & 0 & \phi & -\phi - \frac{1}{\tau_f} - b & b & 0 & 0 \\ \gamma^3 / \tau_f & 0 & 0 & \phi & -\alpha K - \frac{1}{\tau_f} - b & b & 0 \\ \gamma^4 / \tau_f & 0 & 0 & 0 & \alpha K & -b - \frac{1}{\tau_f} - W & 0 \\ 0 & 0 & 0 & 0 & 0 & W & 0 \end{bmatrix} \quad (\text{A4})$$

But eqs. (A1) are not linear. The first order perturbation approximation is adapted and we can linearize (with bar denoting average) to get $\mathbf{c} = \bar{\mathbf{c}} + \delta\mathbf{c}$.

$$\delta\dot{\mathbf{c}} = \mathbf{A}'\delta\mathbf{c}, \quad \delta\mathbf{c} = [\delta L_f, \delta C_0, \delta C_1, \dots, \delta C_N, p_f] \quad (\text{A5})$$

where \mathbf{A}' is

$$\mathbf{A}' = \begin{bmatrix} -\kappa R - \sum_{j=1}^4 \gamma^j / \tau_f & \frac{1}{\tau_f} & \frac{1}{\tau_f} & \frac{1}{\tau_f} & \frac{1}{\tau_f} & \frac{1}{\tau_f} & 0 \\ \kappa R & -\frac{1}{\tau_f} - \phi & \frac{1}{b} & 0 & 0 & 0 & 0 \\ \gamma / \tau_f & \phi & -\phi - \frac{1}{\tau_f} - b & b & 0 & 0 & 0 \\ \gamma^2 / \tau_f & 0 & \phi & -\phi - \frac{1}{\tau_f} - b & b & 0 & 0 \\ \gamma^3 / \tau_f & 0 & 0 & \phi + \frac{\alpha K \sigma C_3}{\epsilon + \sigma(C_2 + D_2)} & -\alpha K - \frac{1}{\tau_f} - b & b & 0 \\ \gamma^4 / \tau_f & 0 & 0 & -\frac{\alpha K \sigma C_3}{\epsilon + \sigma(C_2 + D_2)} & \alpha K & -b - \frac{1}{\tau_f} - W & 0 \\ 0 & 0 & 0 & 0 & 0 & W & 0 \end{bmatrix} \quad (\text{A6})$$

Applying the Laplace transform, $\delta\mathbf{C}(s) = \int_0^\infty \delta\mathbf{c}e^{-st} dt$, the master equations can be rewritten as:

$$(s - \mathbf{A})\delta\mathbf{C}(s) = \delta\mathbf{c}(t=0) = [1, \dots, 0]^T \quad (\text{A7})$$

The MFPT can be written:

$$T = \int_0^\infty t p_f(t) dt = -\frac{d}{ds} \int_0^\infty p_f(t) e^{-st} dt \Big|_{s=0} = -W \frac{d\delta C_N(s)}{ds} \Big|_{s=0} \quad (\text{A8})$$

which can be calculated numerically. It should be notified that the concentration and probability have the same master equations but a different pre-factor. When choosing the initial condition $[1, \dots, 0]^T$, the pre-factor is set to be 1 and $\delta C_N(s)$ solved from eq. (A7) is exactly a probability distribution .

Appendix B: Simulation Details for Phase Diagram

In this figure, we run 10^6 samples with random sets log uniformly choosen between $\gamma \in [10^{-4}, 10]$, $\phi \in [10^{-10}, 10^{10}]s^{-1}$, $b \in [10^{-15}, 10^{15}]s^{-1}$.

It can be observed that a large amount of red points distributes over regimes C and D with $\eta \sim 100$. This is because of $\gamma \sim 10$ and the inverse flux at the final step dominates. In the extreme case: b/ϕ is very large, $C_0 \simeq D_0$ will occupy most of products and free ligands L_s, L_f have little concentration.

$$\frac{L_s}{L_f} = \frac{D_0 \tau_s^{-1}}{C_0 \tau_f^{-1}} = \frac{\tau_s^{-1}}{\tau_f^{-1}}$$

As γ^N/τ_i dominates,

$$\eta = \frac{D_N}{C_N} = \frac{L_s \gamma^N / \tau_s}{L_f \gamma^N / \tau_f} = \frac{\tau_f^2}{\tau_s^2} = 100$$

Appendix C: Changing the number of phosphorylation steps

Here, we show simulations for the KPR-cascade when we vary the maximum number of phosphorylation steps N .

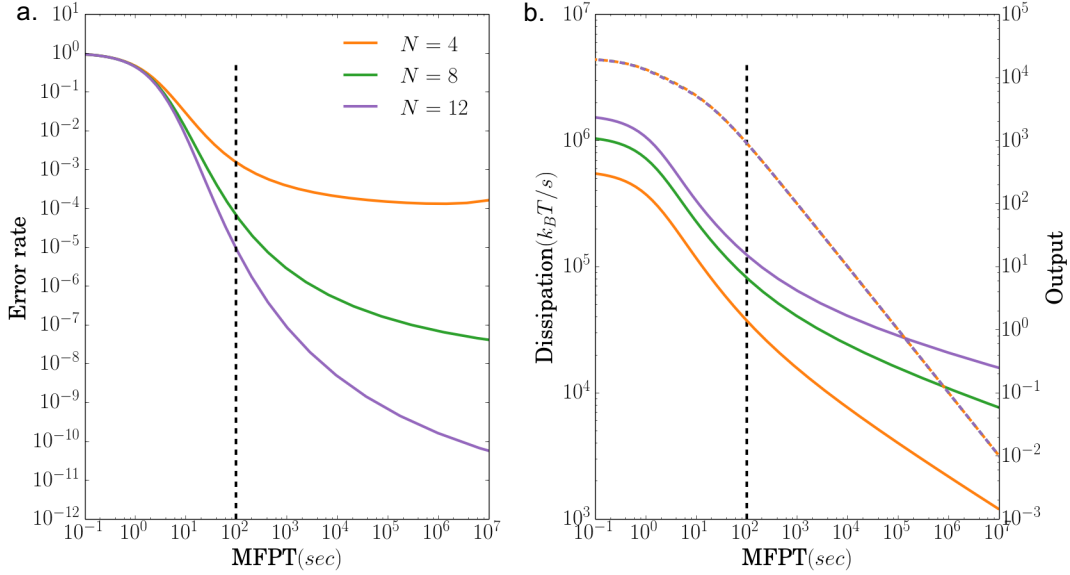


FIG. 6. Effects of the step size N in KPR: $\tau_s = 1s$, $\tau_f = 10s$, we change ϕ but keep $b/\phi = 0.01$, $\gamma = 10^{-3}$ fixed. The lines are for $N = 4, 8$ and 12 . The vertical black dashed line is for time = $100s$. (a): relation between accuracy and speed; (b): relation between dissipation(solid)/output(dashed) and speed.

* pankajm@bu.edu

- [1] D. J. Irvine, M. A. Purbhoo, M. Krogsgaard, and M. M. Davis, *Nature* **419**, 845 (2002).
- [2] A. K. Chakraborty and A. Weiss, *Nature immunology* **15**, 798 (2014).
- [3] S. Stoll, J. Delon, T. M. Brotz, and R. N. Germain, *Science* **296**, 1873 (2002).
- [4] T. W. McKeithan, *Proceedings of the national academy of sciences* **92**, 5042 (1995).
- [5] U. Alon, *An introduction to systems biology: design principles of biological circuits* (CRC press, 2006).
- [6] O. Feinerman, R. N. Germain, and G. Altan-Bonnet, *Molecular immunology* **45**, 619 (2008).
- [7] P. François and G. Altan-Bonnet, *Journal of Statistical Physics* **162**, 1130 (2016).
- [8] N. R. Gascoigne, T. Zal, and S. M. Alam, *Expert reviews in molecular medicine* **3**, 1 (2001).

- [9] P. Sartori and S. Pigolotti, *Physical Review X* **5**, 041039 (2015).
- [10] J. J. Hopfield, *Proceedings of the National Academy of Sciences* **71**, 4135 (1974).
- [11] J. Ninio, *Biochimie* **57**, 587 (1975).
- [12] M. Lever, P. K. Maini, P. A. Van Der Merwe, and O. Dushek, *Nature Reviews Immunology* **14**, 619 (2014).
- [13] P. François and E. D. Siggia, *Physical biology* **5**, 026009 (2008).
- [14] J.-B. Lalanne and P. François, *Physical review letters* **110**, 218102 (2013).
- [15] P. François, G. Voisinne, E. D. Siggia, G. Altan-Bonnet, and M. Vergassola, *Proceedings of the National Academy of Sciences* **110**, E888 (2013).
- [16] M. A. Savageau and R. R. Freter, *Biochemistry* **18**, 3486 (1979).
- [17] M. Ehrenberg and C. Blomberg, *Biophysical journal* **31**, 333 (1980).
- [18] R. R. Freter and M. A. Savageau, *Journal of theoretical biology* **85**, 99 (1980).
- [19] H. Qian, *Journal of molecular biology* **362**, 387 (2006).
- [20] A. Murugan, D. A. Huse, and S. Leibler, *Proceedings of the National Academy of Sciences* **109**, 12034 (2012).
- [21] R. Rao and L. Peliti, *Journal of Statistical Mechanics: Theory and Experiment* **2015**, P06001 (2015).
- [22] P. Mehta, A. H. Lang, and D. J. Schwab, *Journal of Statistical Physics* **162**, 1153 (2016).
- [23] R. Landauer, *IBM journal of research and development* **5**, 183 (1961).
- [24] W. Bialek and S. Setayeshgar, *Proceedings of the National Academy of Sciences of the United States of America* **102**, 10040 (2005).
- [25] T. Mora, *Physical review letters* **115**, 038102 (2015).
- [26] A. H. Lang, C. K. Fisher, T. Mora, and P. Mehta, *Physical review letters* **113**, 148103 (2014).
- [27] S. B. Laughlin, *Current opinion in neurobiology* **11**, 475 (2001).
- [28] H. Qian, *Biophysical chemistry* **105**, 585 (2003).
- [29] G. Lan, P. Sartori, S. Neumann, V. Sourjik, and Y. Tu, *Nature physics* **8**, 422 (2012).
- [30] S. Lahiri, J. Sohl-Dickstein, and S. Ganguli, *arXiv preprint arXiv:1603.07758* (2016).
- [31] T. L. Hill, *Free energy transduction and biochemical cycle kinetics* (Springer Science & Business Media, 2012).
- [32] H. Qian, *Annu. Rev. Phys. Chem.* **58**, 113 (2007).
- [33] V. Srivastava and N. E. Leonard, in *2015 American Control Conference (ACC)* (IEEE, 2015) pp. 2113–2118.
- [34] G. Bel, B. Munsky, and I. Nemenman, *Physical biology* **7**, 016003 (2009).
- [35] P. B. Detwiler, S. Ramanathan, A. Sengupta, and B. I. Shraiman, *Biophysical Journal* **79**, 2801 (2000).
- [36] N. G. Van Kampen, *Stochastic processes in physics and chemistry*, Vol. 1 (Elsevier, 1992).
- [37] P. Mehta and D. J. Schwab, *Proceedings of the National Academy of Sciences* **109**, 17978 (2012).
- [38] S. K. Kim, *The Journal of Chemical Physics* **28**, 1057 (1958).
- [39] N. Barkai and S. Leibler, *Nature* **387**, 913 (1997).
- [40] W. Ma, A. Trusina, H. El-Samad, W. A. Lim, and C. Tang, *Cell* **138**, 760 (2009).
- [41] P. Francois, M. Hemery, K. A. Johnson, and L. N. Saunders, *Physical Biology* **13**, 066011 (2016).
- [42] T. D. Pollard and G. G. Borisy, *Cell* **112**, 453 (2003).
- [43] R. Milo, P. Jorgensen, U. Moran, G. Weber, and M. Springer, *Nucleic acids research* **38**, D750 (2010).
- [44] J. Rosing and E. Slater, *Biochimica et Biophysica Acta (BBA)-Bioenergetics* **267**, 275 (1972).
- [45] W. Bialek, *Biophysics: searching for principles* (Princeton University Press, 2012).
- [46] A. K. Chakraborty and J. Das, *Nature Reviews Immunology* **10**, 59 (2010).
- [47] R. J. Brownlie and R. Zamoyska, *Nature Reviews Immunology* **13**, 257 (2013).
- [48] I. Štefanová, B. Hemmer, M. Vergelli, R. Martin, W. E. Biddison, and R. N. Germain, *Nature immunology* **4**, 248 (2003).
- [49] A. Murugan, D. A. Huse, and S. Leibler, *Physical Review X* **4**, 021016 (2014).
- [50] J. M. Lemons, X.-J. Feng, B. D. Bennett, A. Legesse-Miller, E. L. Johnson, I. Raitman, E. A. Pollina, H. A. Rabitz, J. D. Rabinowitz, and H. A. Collier, *PLoS Biol* **8**, e1000514 (2010).
- [51] H. S. Zaher and R. Green, *Cell* **136**, 746 (2009).
- [52] J. D. Roberts, K. Bebenek, and T. A. Kunkel, *Science* **242**, 1171 (1988).
- [53] Y. Tu, *Proceedings of the National Academy of Sciences* **105**, 11737 (2008).
- [54] S. Vaikuntanathan, T. R. Gingrich, and P. L. Geissler, *Physical Review E* **89**, 062108 (2014).
- [55] A. Murugan and S. Vaikuntanathan, *arXiv preprint arXiv:1605.08407* (2016).
- [56] C. Blomberg *et al.*, *Journal of theoretical biology* **88**, 631 (1981).
- [57] B. Hu, W. Chen, W.-J. Rappel, and H. Levine, *Physical review letters* **105**, 048104 (2010).